On the formation of a sticking layer on the bearing during thin – section aluminium extrusion

X. Ma[1*], M.B. de Rooij [2] and D.J.Schipper [3]
[1] Materials Innovation Institute, The Netherlands
[2,3] University of Twente, Laboratory of Surface Technology & Tribology, The Netherlands
*Corresponding author. Postal address: De Horst, University of Twente, 7500 AE, P.O.Box 217, The Netherlands. Email: x.ma@m2i.nl

Abstract: This paper describes the use of Comsol Multiphysics to determine the shear layer thickness in thin – section aluminium extrusion, based on the minimum work criterion. The studied two aluminium alloys are AA 6063 and AA 7020. The results show that a continuous shear layer featuring shear localisation due to localised thermal softening is not possible to form under typical thin – section aluminium extrusion conditions.

Keywords: Aluminium extrusion; FEM; Comsol

1. Introduction

In aluminium extrusion processes, near the bearing entrance an aluminium sticking layer can be found on the bearing surface in the die [1-3]. The formation of this layer is closely related to the large friction forces between the bearing and extrudate near the entrance of the bearing. Close to the bearing exit, friction is reduced and no sticking layer is formed. However, the exact formation mechanism remains unclear. Two mechanisms could be relevant: 1) that an aluminium shear layer is formed at the interface of steel and bulk aluminium. Since the exiting extrudate has a constant velocity profile through the thickness, this layer must be deposited on the steel surface, similar to the formation of secondary deformation zone found in cutting processes; 2) that no complete shear layer is formed, but discrete patches of aluminium adhere to the bearing asperities and under the stress conditions eventually form a complete layer. For the first formation mechanism, since all the shear strain is confined within a thin shear layer, the problem is a strain localisation problem that has been analysed by several researchers. The general condition for this layer is that a local increase in plastic strain rate in a weaker region leads to an increase in temperature and consequently to a further increase in strain-rate. Most of the analytical solutions that calculate the thickness of this shear layer assume that this layer forms under adiabatic conditions [4-7]. Specifically focused on shear layer found in turning processes, Oxley and Hastings developed a theoretical model that was also experimentally validated, and they proved that the plastic shear layer thickness is determined by a minimum work criterion, its value being such that for certain boundary conditions the total work done in shearing layer will be minimised. In this study a FEM model has been built in Comsol Multiphysics, based on this criterion, to examine whether such a layer can be formed in the bearing channel during extrusion of AA 6063 and AA 7020, and if it can, to determine its thickness.

Nomenclatures

d	Half thickness of the aluminium extrudate	[m]
r_{stl}	Radius of the tooling that surrounds the extrudate (die + outer ring)	[m]
δ	Ratio between the shear layer thickness and half of the extrudate thickness	[-]
x	Through – thickness location	[m]
v	Extrusion velocity	[m/s]
$\dot{\varepsilon}$	Strain rate in the aluminium extrudate	[1/s]
T	Temperature in the aluminium extrudate	[K]
t	Analysis time in the transient analysis	[s]

ρ_{al}	Density of aluminium extrudate	[kg/m^3]
c_{al}	Specific heat capacity of aluminium extrudate	[J/(kg·K)]
k_{al}	Thermal conductivity of aluminium extrudate	[W/(m·K)]
k_{stl}	Thermal conductivity of steel die	[W/(m·K)]
σ	Flow stress of aluminium extrudate	[Pa]
s_m	Constant in Sellars-Tegart constitutive relation for aluminium alloys	[Pa]
A	Constant in Sellars-Tegart constitutive relation for aluminium alloys	[1/s]
Q	Constant in Sellars-Tegart constitutive relation for aluminium alloys	[J/mol]
R	Universal gas constant	[J/(mol·K)]
m	Constant in Sellars-Tegart constitutive relation for aluminium alloys	[-]
h_{stl-al}	Heat transfer coefficient between die and extrudate	[W/(m^2·K)]
h_{stl-a}	Heat transfer coefficient between die and air	[W/(m^2·K)]
T_{int_al}	Extrudate temperature at the die-aluminium interface	[K]
T_{int_stl}	Bearing temperature at the die-aluminium interface	[K]
T_{stl-a}	Outer ring temperature at the outer ring – air interface	[K]
T_a	Air temperature	[K]
P	Total power for shearing the shear layer per unit length and width	[W/m^2]
P_{max}	Maximum total power as the normalising factor	[W/m^2]
n	Strain rate sensitivity in the linear thermal softening equation	[-]
a	Thermal softening parameter	[-]
σ_0	Reference stress in the linear thermal softening equation	[Pa]
T_0	Reference temperature in the linear thermal softening equation	[K]
$\dot{\varepsilon}_0$	Reference strain rate in the linear thermal softening equation	[1/s]

2. The Model

2.1 Model formulation

The primary assumptions for the mathematical formulation are: 1) Due to standard industrial practise – preheating of the die, it is assumed that once the extrusion starts, the die reaches thermal equilibrium, i.e., the die temperature is determined by the extrudate temperature in contact; 2) Only radial heat conduction in the die is considered; 3) Heat conduction in extrusion direction is negligible compared to radial direction. The model is also highly geometry dependent therefore only a typical thin section extrusion set up was considered, i.e., the thickness of the extrudate profile is small compared to the bearing length.

For thin-section extrudate flowing out inside the bearing channel, if a shear layer can be developed along the interface between the extrudate and the die bearing, since its thickness and the length of the sticking zone are both small, it is reasonable to assume that the layer thickness is constant along the bearing. So the velocity of the extrudate only depends on location through the extrudate thickness [7], not on the location on the bearing in the extrusion direction. In the calculations, triangular strain rate distribution is assumed. Suppose half of the thickness of the extrudate is ***d*** and the thickness of the shear layer is δd, as shown in Fig. 1. The above assumptions result in the following velocity and strain rate profiles in the extrudate [8].

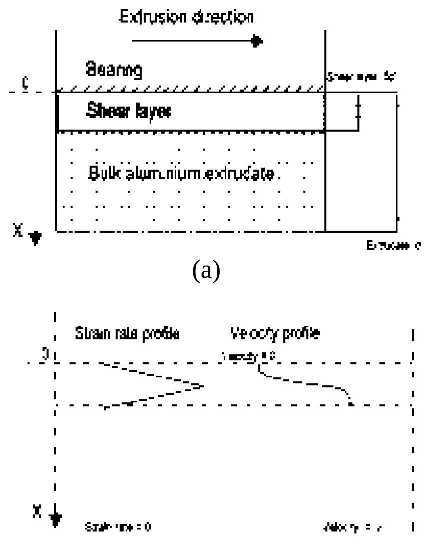

(a)

(b)

Figure **1** Schematic view of the studied domain: (a) Shear layer; (b) Schematic view of the assumed strain rate and velocity profile with no wall slip.

If heat conduction along the extrusion direction can be neglected compared to the x direction heat conduction, the 2 – D rectangular domain can be simulated by a transient 1-D problem (which also ensures that convective heat transfer is taken into account) that models the passing of a through-thickness aluminium element. In the aluminium extrudate subdomain:

$$\dot{g} = \begin{cases} 4xv/d^2d^2 & 0 \le x \le dd/2 \\ 4v(dd-x)/d^2d^2 & dd/2 \le x < dd \\ 0 & x \ge dd \end{cases} \qquad (1)$$

The energy equation in the aluminium extrudate domain now writes:

$$r_{al}c_{al}\frac{\partial T}{\partial t} = k_{al}\frac{\partial^2 T}{\partial x^2} + fs\dot{g} \qquad (2)$$

Where f is the heat generation rate taken as 0.9 [9]. Heat is generated in the shear layer due to the shear deformation. At the interface between die and extrudate, heat is exchanged by an effective heat transfer coefficient $h_{stl\text{-}al}$ that takes into account the little gap between the two due to interface roughness. Therefore at the die – aluminium interface:

$$-k_{al}\frac{\partial T}{\partial x} = h_{stl-al}\left(T_{int\_al} - T_{int\_stl}\right) \qquad (3)$$

$$-k_{stl}\frac{\partial T}{\partial x} = h_{stl-al}\left(T_{int\_stl} - T_{int\_al}\right) \qquad (4)$$

At the die – air interface, heat is exchanged by heat transfer from the die to the air:

$$-k_{stl}\frac{\partial T}{\partial x} = h_{stl-a}\left(T_{stl-a} - T_a\right) \qquad (5)$$

Where the surrounding air temperature T_a was fixed at 25 °C. In the die subdomain there is no convective heat transfer, therefore it is not part of the transient heat transfer modelling. Instead, a steady-state is assumed and only radial heat conduction as a result of the heat generating aluminium extrudate is considered. Considering heat conduction and boundary conditions (4) and (5) applied to a cylindrical die set (die + outer ring), the bearing temperature only depends on the thermal conductivity of steel, the heat transfer coefficients at the die – aluminium interface and at the die – air interface, and the aluminium extrudate temperature at the interface. The bearing temperature thus writes:

$$T_{int\_stl} = \frac{h_{stl-a}T_{int-al} + h_{stl-al}T_a\left(\frac{d}{r_{stl}} + \frac{h_{stl-al}r_{stl}}{k_{stl}}\right)}{h_{stl-a} + h_{stl-al}\left(\frac{d}{r_{stl}} + \frac{h_{stl-al}r_{stl}}{k_{stl}}\right)} \qquad (6)$$

Combining equation (3) and (6) the boundary condition at the die – aluminium interface is set up. Given parameters the extrusion speed v and the ratio of shear layer thickness and half extrudate thickness, the problem is fully defined.

2.2. Minimum work criterion

The above analysis is fully defined once parameter δ is chosen. The real choice of δ is determined such that it minimises the total work done in the shearing process, as proposed by Oxley and Hastings in their studies of the thickness of the secondary deformation zone at the chip – tool interface [10]. In this study the total work rate (power) was calculated instead of the total work.

Aluminium alloys demonstrate both thermal softening and strain rate hardening constitutive behaviour. The combined effects of both can be modelled using the Sellars – Tegart law [2]:

$$s(T,\dot{g}) = s_m\left[\left(\frac{\dot{g}}{A}\exp\left(\frac{Q}{RT}\right)\right)^{\frac{1}{m}}\right] \qquad (7)$$

The flow stress of aluminium alloys AA 6063 and AA 7020 is shown in Figure 2. For any metal that is softened by temperature but hardened by strain rate or strain, a thin shear layer leads to great strain rate hardening in the shear zone, which also increases thermal softening as a result. These two competing effects result in a minimum in the flow stress curve as a function of different thicknesses of the shear layer which minimises the total work done in the shearing process [10].

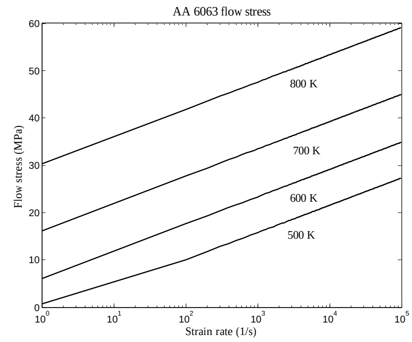

(a)

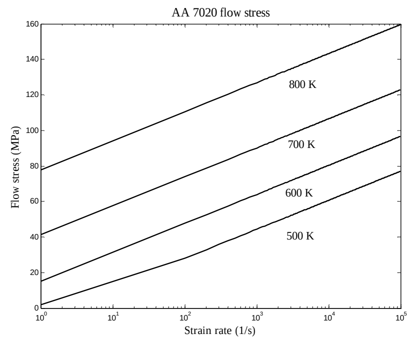

(b)

Figure **2** Effect of temperature and strain rate on flow stresses of aluminium alloys: (a) AA 6063 (b) AA 7020

For a certain δ value, the temperature distribution through the layer thickness can be obtained. The total power per length per width (as for the one dimensional nature of the problem) needed to realise the localised deformation in the shear zone can be obtained as follows, considering the strain rate profile as depicted in Fig. 1(b).

$$P = \int_0^{\delta d} \sigma(x)\dot{\gamma}(x)dx = \frac{4v}{\delta^2 d^2}\left(\int_0^{\delta d/2} \sigma(x)x\,dx + \int_{\delta d/2}^{\delta d} \sigma(x)(\delta d - x)dx\right) \quad (8)$$

In this equation, the flow stress $\sigma(x)$ is a function of temperature and strain rate at the through – thickness location x. Therefore, the thickness of this shear layer at a certain extrusion speed will be determined such that its corresponding parameter δ minimises the total power for shearing the layer. The practical range of δ is 0 – 0.2, since a shear layer thickness larger than that cannot be formed as that constitutes bulk deformation [10].

2.3 FEM modelling

The FEM model was built in Comsol Multiphysics v3.5 using the 1-D transient heat conduction module that calculates temperature distribution in a through – thickness element, when it is passing the bearing area. The transient nature ensures that the convective heat transfer by extrudate leaving the bearing area and new extrudate entering the die at the die entrance is taken into account. The modelled extrudate domain can be shown as below:

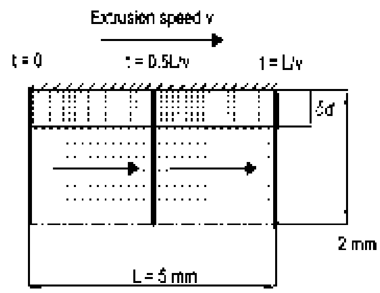

(a)

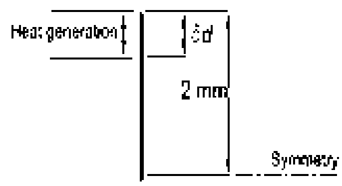

(b)

Figure **3** FEM modelling of the problem: (a) 2-D problem (b) Schematic view of the modelled 1-D aluminium element

The geometrical specifications are shown as below:

Table **1** Geometry of modelled domain

Parameters	Value	Unit
d	2	mm
r_{stl}	20	mm
L	5	mm

The parameters in equation (7) that define the flow stress of AA 6063 and AA 7020 (as shown in Fig.2) are listed below in Table 2 [2]:

Table **2** Parameters used in the Sellars – Tegart equations of AA 6063 and AA 7020

Alloys	s_m (MPa)	A (1/s)	Q (J/mol)	R (J/(mol*K))	m
AA 6063	25	$5.91*10^9$	$1.41*10^5$	8.31	5.39
AA 7020	70.9	$1.03*10^9$	$1.29*10^5$	8.31	5.41

Subdomain properties used are listed below**:**

Table **3** Subdomain properties

Materials	ρ (kg/m^3)	c (J/(Kg*K))	k (W/(m*K))
AA 6063	2700	897	300
AA 7020	2700	897	300
Tool steel	7980	450	25

Boundary conditions are listed in Table 4:

Table **4** Boundary conditions used in the FEM modelling

Boundaries	Type	Value
Die – air	Heat transfer coefficient	110 W/(m^{2}K) [11]
Die – aluminium	Effective heat transfer coefficient	11000 W/(m^{2}K) [11]
Symmetry plane	Temperature gradient	0 K/m

Initial temperature of the extrudate (thus temperature of extrudate entering the die) was taken as 800 K to simulate the aluminium extrudate that just gets out of the deformation zone. The domain calculation time was taken as the characteristic time of the problem in which the element passes the bearing. The extrusion speed was varied from 0.2 m/s to 10 m/s. The shear layer thickness ratio δ was varied from 0 to 0.2. The objective of the modelling is to find a minimum in the total power curve as a function of shear zone thickness that determines the real thickness of this shear layer abovementioned.

3. Results

The assumption in the one dimensional analysis is that the heat conduction in the extrusion direction was neglected. This is the case if the conductive heat flux in extrusion direction is negligible compared to that in the thickness direction. The average conductive heat fluxes in both directions were calculated after FEM computation to determine whether such an assumption was reasonable. The average conductive heat flux in the extrusion direction was calculated by relating the difference between average through-thickness temperatures at the solution time and at the initial condition; the average conductive heat flux in the through-thickness direction was calculated by relating the temperature difference between the die-aluminium interface (A) and the symmetry plane. The results for AA 6063 are shown in Fig.4:

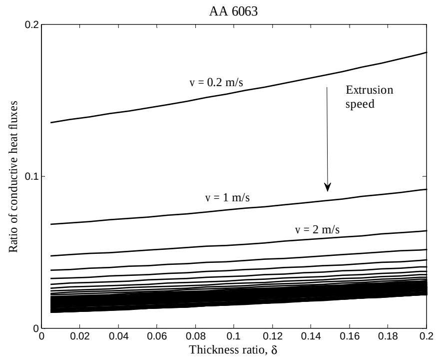

Figure **4** Ratio of conductive heat fluxes in the extrusion direction over the through – thickness direction for AA 6063 simulation.

It is clear that as extrusion speed increases from the lowest speed 0.2m/s, this ratio is decreased from about 0.15 quite rapidly to around 0.03. AA 7020 shows very similar results. This suggests that the assumption that the heat conduction in the extrusion direction is indeed negligible to that in the radial direction is reasonable, which results in one dimensional heat conduction in the radial direction; so the only heat transfer in the extrusion direction is the convective heat transfer as a result of the mass of aluminium flowing out of the bearing. However, this assumption breaks down if the profile is not of a thin-section type (section thickness larger than bearing length), in which the conductive heat flux in the radial direction is comparable to that of the extrusion direction.

The following graphs show how the total power needed to shear the layer varies with the thickness ratio δ and the extrusion speed for both aluminium alloys studied. The total power shown below has been normalised by the maximum value at each velocity:.

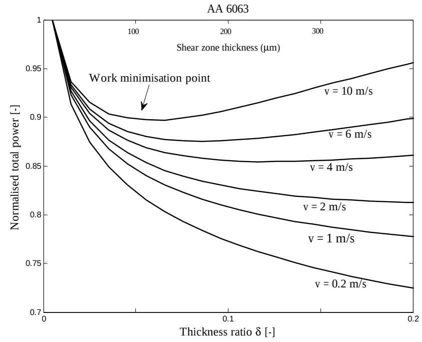

(a)

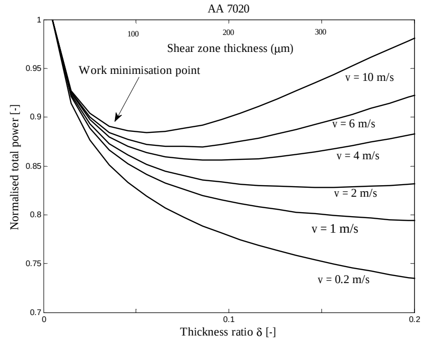

(b)

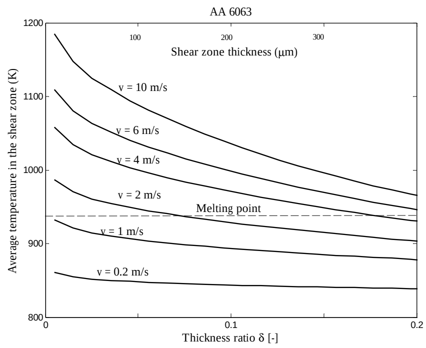

(c)

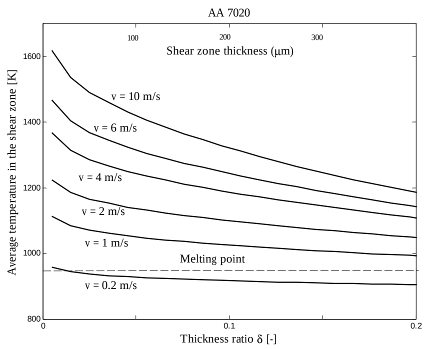

(d)

Figure **5** Results of the FEM simulation: (a) Normalised total power of AA 6063 as a function of thickness ratio and extrusion speed; (b) Normalised total power of AA 7020 as a function of thickness ratio and extrusion speed; (c) Average temperature in the shear layer of AA 6063; (d) Average temperature in the shear layer of AA 7020.

The maximum power needed in each velocity P_{max} calculated is shown in Table 5:

Table **5** Maximum power calculated for 2 alloys

AA 6063		AA7020	
v [m/s]	P_{max} [W/m^2]	v [m/s]	P_{max}[W/m^2]
0.2	1.0*10^7	0.2	2.4*10^7
1	5.1*10^7	1	1.1*10^8
2	9.8*10^7	2	2.1*10^8
4	1.9*10^8	4	4.0*10^8
6	2.7*10^8	6	5.7*10^8
10	4.4*10^8	10	9.0*10^8

It can be seen in Figure 5, as the thickness ratio increases, the strain rate is reduced, leading to less strain rate hardening; in the mean time, this reduction in strain rate decreases the heat generation therefore the average temperature in the shear layer is decreased, leading to less thermal softening. As for the shear layer thickness as determined by looking for a minima in the total work rate curve, however, the combined effects of thermal softening and strain rate hardening results in: 1) for AA 6063, the minima in the total work rate curve expected cannot be found in the studied domain for extrusion speeds lower than 4 m/s. When the extrusion speeds are higher than this value, this minima is present at the thickness ratio around 0.05 – 0.1, and this thickness generally decreases when the extrusion speed increases; 2) for AA 7020, likewise, the minima cannot be found for extrusion speeds lower than 1m/s; When the extrusion speeds are higher than this value, this minima is present at the thickness ratio around 0.05 – 0.2, and this thickness decreases as extrusion speed increases.

The reasons that a minimum cannot be found at low extrusion speed are: 1) The strain rate sensitivity is high compared to the thermal softening effect, therefore the average flow stress is high despite the high temperature and thus total power in the shearing process keeps decreasing once the strain rate decreases as the thickness of the shear layer increases, leading to a superplastic-like behaviour that hinders localised shearing; 2) At slow extrusion speeds the heat generation in the shear layer is small, and the effect of thermal softening is outnumbered by that of the strain rate hardening; at high extrusion speeds the heat generation is big enough to generate enough heat to soften the shear layer material. For AA 6063 and AA 7020, the similarity in the curve is a result of similar strain rate sensitivity (see Table 1). The relative easiness of AA 7020 to form a shear layer is due to the fact that its flow stress is much higher than AA 6063 (see Figure 2) and that heat generation is large enough to soften the material at a lower speed. Dinzart and Molinari's analytical model [7] that studied the formation of an adiabatic shear localisation region suggests the same conclusions: the thickness of the shear layer generally depends on material's constitutive properties; its thickness increases with strain rate sensitivity but decreases with thermal softening sensitivity; it also decreases with sliding speed.

However, as the curve tells us, is the shear layer thickness found at high extrusion speeds practical? The temperature curves in Figure 5 (c) and (d) show that for AA 6063 extrusion, when the extrusion speed is higher than 1 m/s, the temperature in the shear layer is above the melting point, which is impractical. AA 7020 has a narrower process window as the heat generation is greater with this material. When the extrusion speed is higher than 0.4m/s, the surface starts to melt. Therefore, the observation here that a shear layer can be developed at high extrusion speeds for both AA 6063 and AA 7020 is not practical.

4. Conclusions

A one dimensional FEM model was built in Comsol Multiphysics to determine the thickness of the shear layer at the die – extrudate interface in aluminium extrusion of AA 6063 and AA 7020, using a work minimum criterion as proposed by Oxley and Hastings. The results suggest that the thickness of this shear layer depends on material's constitutive properties: it increases with strain rate sensitivity but decreases with thermal softening sensitivity and sliding speed. The analysis on AA 6063 and AA 7020 suggests that in thin – wall extrusion processes operated in practical process window, the strain-confining shear layer cannot develop due to high strain rate sensitivity and relatively low thermal softening. Therefore the sticking layer found on the die in aluminium extrusion is formed by discrete sticking mechanism, rather than continuous shearing from the bulk flow.

5. Acknowledgement

This research was carried out under the project number MC 4.05218 in the framework of the Research Program of the Materials innovation institute M2i (www.m2i.nl), which is greatly appreciated.

6. References

[1] Tverlid, S., Modelling of friction in the bearing channel of dies for extrusion of aluminium sections, *PhD Thesis Norwegian University of Science and Technology, N-7034 Trondheim*, Norway, 1998.

[2] Sheppard, T., Extrusion of Aluminium Alloys, Kluwer Academic Publishers, The Netherlands, 1999.

[3] Abtahi, S., Interface mechanisms on the bearing surface in extrusion, *7th International Aluminium Extrusion Technology Seminar*.

[4] Fressengeas and C., Molinari, A., Instability and localization of plastic flow in shear at high strain rates, *J.Mech.Phys.Solids*, **35**, 1987, pp. 185.

[5] Wright, T.W. and Ockendon, H., A model for fully formed shear bands, *J.Mech.Phys.Solids*, **40**, 1992, pp. 1217.

[6] Molinari, A. and Musquar, C. and Sutter, G., Adiabtic shear banding in high speed machining of Ti-6Al-4V:experiments and modelling, *International Journal of Plasticity*, **18**, 2002, pp.443.

[7] Dinzart, F. and Molinari, A., Structure of adiabatic shear bands in thermo-viscoplastic materials, *Eur.J.Mec*, A/Solids, **17**, 1998, pp.923.

[8] Qi, H.S. and Mills, B., Formation of a transfer layer at tool – chip interface during machining, *Wear*, **245**, 2000, pp.136.

[9] Schmitter, E.D., Modelling massive forming processes with thermally coupled fluid dynamics, *Proceedings of the COMSOL*

Multiphysics User's Conference, 2005, Frankfurt.
[10] Oxley, P.L.B. and Hastings, W.F., Minimum work as a possible criterion for determining the frictional conditions at the tool/chip interface in machining, *Philosophical Transations of The Royal Society A*, **282**, 1976, pp 565.
[11] Li,L., Zhou, J and Duszczyk, J., Prediction of temperature evolution during the extrusion of 7075 aluminium alloy at various ram speeds by means of 3D FEM simulation, *Journal of Materials Processing Technology*, **145**, 2004, pp.360